FRACTAL BEHAVIOR OF FRACTURE SURFACES OF 15-5PH STEEL

Kamila Amato de Campos, kamila_ac@hotmail.com
Celso Yoshino, celso.yoshino@uol.com.br
São Paulo State University, Materials and Technology Department, Guaratinguetá Campus, Av. Ariberto Pereira da Cunha, 333, 12516-410,Guaratinguetá, SP, Brazil

Luis Rogerio de Oliveira Hein, rhein@feg.unesp.br
São Paulo State University, Materials and Technology Department, Guaratinguetá Campus, Av. Ariberto Pereira da Cunha, 333, 12516-410,Guaratinguetá, SP, Brazil

Abstract. *The topography of fracture surface along stretch zone for 15-5PH steel is analyzed for different specimen thicknesses, providing a range in elastic-plastic behavior. The relationship between stretch zone width, as a local toughness measurement, and fractal dimension is discussed about the restrictions imposed by stress field evolution. The image stacks were acquired using a reflected light microscope for extended depth-of-field 3-D reconstruction. Stretch zone regions were delimited from elevation maps using a tablet. Each elevation map was divided in three rectangular areas of same size, since the stretch zone was enclosed. This procedure avoids a large variation on stretch zone width measurements, computed as the mean value for all line segments inside stretch zone. Same rectangular areas were considered for fractal dimension measurements. Stretch zone fractal dimension data were computed using another plugin for NIH Image J, the "Map Fractal Count", based on the Minkowski-Bouligand dimension method, also known as box-counting dimension, which systematically lay a series of grids of decreasing box size over the grayscale elevation map and record the number of boxes for each successive grid size, finding the fractal dimension D as the slope of the logarithmic regression line for box numbers and grid sizes. In all measured values for stretch zone width and fractal dimension for all analyzed regions in each specimen observed that there is a significant correlation between stretch zone width and fractal dimension with specimen thickness. It demonstrates that stretch zone has heterogeneous topographic behavior along thickness. And, finally, a general equation is suggested to describe stretch zone width dependence on fractal dimension and thickness.*

Keywords*: quantitative fractography; stretch zone; fractal*

1. INTRODUCTION

The stretch zone is formed under a critical state provided by stable crack propagation in the fracture process in materials with some degree of ductility. In regard to the elastic-plastic fracture process, crack stretching is an important step preceding the real crack initiation phenomenon, which corresponds to the coalescence of the original crack tip with the nearest void (Tarpani *et al.*, 2003). As a fractographic description of blunting before unstable crack propagation, the stretch zone can be related to the local fracture toughness (Landes, 1995). The stretch zone width or height can be related to the critical crack tip opening displacement (CTOD), as it describes the critical stage of fracture process (Pandey *et al.*, 1991) (Das *et al.*, 2006) (Ranganath *et al.*, 1990). The mean topography generated by stretching mechanism can be fitted by a semi parabolic equation (Hein *et al.*, 1999), but this information does not describe the influences of the local stress field and microstructural arrangement. There are some models relating fracture toughness to the fractal dimension values measured from fracture surfaces, but strong discrepancies have been found among them, and the influence of microstructural parameters is often ignored (Charkaluk *et al.*, 1998) (Balakin, 1997).

Fractal dimension is a sensitive parameter for the analysis of features that contribute on fracture surface formation since it is able to describe its behavior, but it is, in fact, a measure of local entropy changes. The property of fractal geometry can be mathematically expressed by concept of self-similarity and self-affinity. The ideal fractal surfaces are nondifferentiable and continuous, presenting the property of self-similarity, or the same behavior at any size scale. Self-affinity is a general scaling transformation, taking anisotropy into account, and should be an adequate framework for the interpretation of the scaling property for structures. Most real fractal surfaces are self-affine due to their intrinsic anisotropy, and this character is found for many fracture surfaces in nature (Horovistiz and Hein, 2005) (Stach *et al.*, 2001).

The aim of this work is to investigate the correlation between fractal dimension and stretch zone width under elastic-plastic conditions and to observe the restrictions in this relationship.

2. EXPERIMENTAL PROCEDURE

According to E1290-93 (ASTM, 2008) the CTOD tests were conducted, using an Instron 8810 servo-hydraulic system. Specimens were cut from a plate of 15-5PH steel. Specimens were machined in four different thicknesses: 9.0 mm, 12.7 mm, 15.0 mm and 19.0 mm.

In each thickness group were selected three valid fractured specimens, for fractographic analysis. Sample surfaces were investigated according to the scheme in Fig. 1, taking image stacks along stretch zone regions at ¼, ½ and ¾ of specimen thickness. The image stacks were acquired using a Nikon Epiphot 200 reflected light microscope equipped with a Diagnostic Instruments Spot Insight Color QE digital camera, adopting 500x magnification in all cases. Images in stacks were pictured for the same axial position of objective lens, taking images at ordered and successive vertical positions, using 1.0 µm intervals. The objective lens was a Nikon ELWD BD/DIC 50x, with numerical aperture of 0.55, lateral resolution of 0.50 µm, depth of field of 1.43 µm, working distance of 8.2 mm and focal length of 4.0 mm.

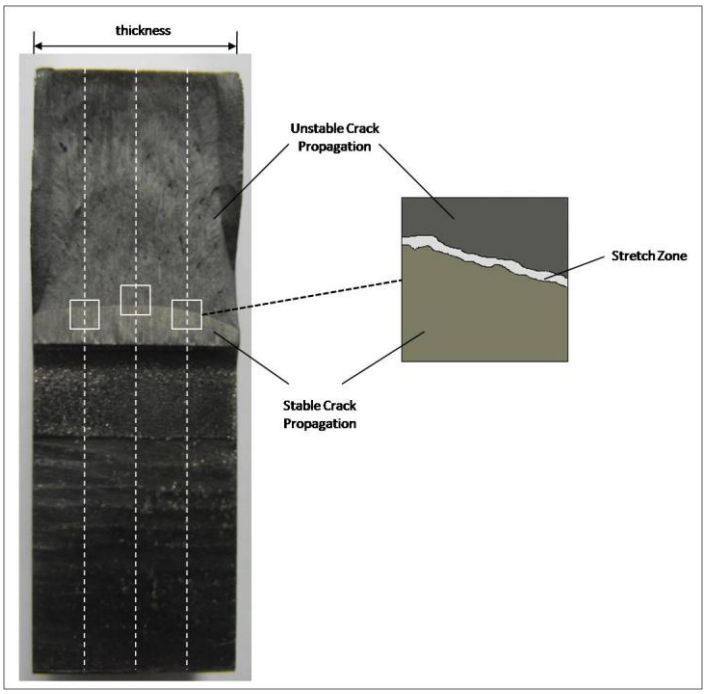

Figure 1. Scheme of the sampling for extended depth-of-field reconstructions

Surface topography maps were obtained by extended depth-of-field reconstruction. This method consists to find the slice with the best in-focus through entire ordered stack, for each x-y image coordinate (Fig. 2a). So, these optima slice positions will be proportional to local elevations that permit to build the corresponding elevation map (Fig. 2b and 2c) (Horovistiz *et al.*, 2003) (Goldsmith, 2000). The chosen extended depth-of-field algorithm is a fusion one that combines images in stack into one single sharp composite, based on the traditional real-valued wavelet transforms (Forster *et al.*, 2004). It was implemented by Prudencio *et al.* (2009) as a plugin program, named as "Extended Depth of Field", for the NIH Image J (Rasband, 2008).

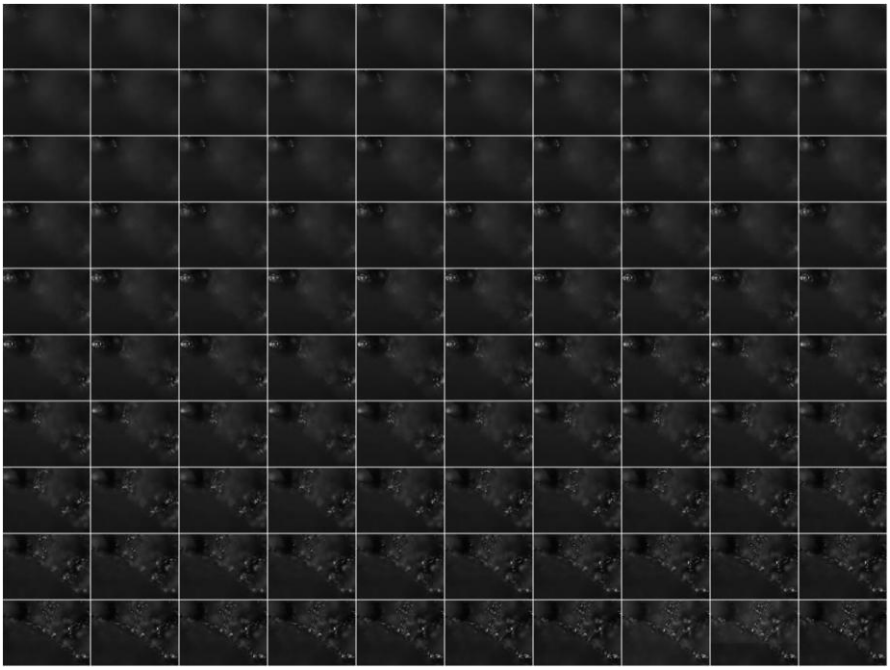

(a)

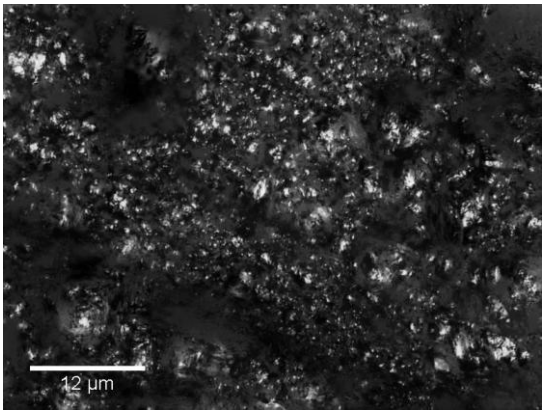

(b)

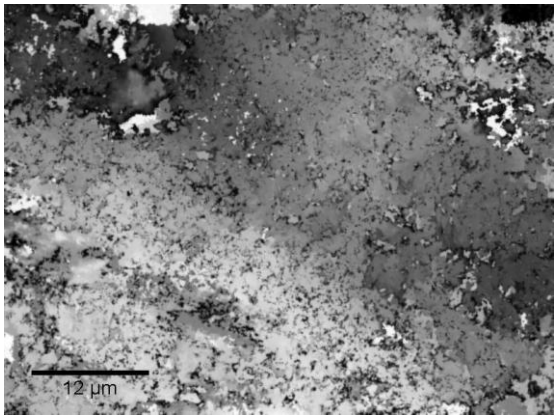

(c)

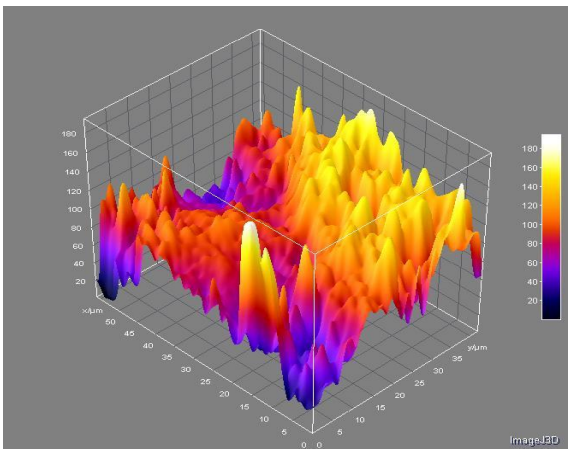

(d)

Figure 2. Extended depth-of-field procedure: (a) images stack; (b) output; (c) elevation map; (d) 3-D representation of image (b)

Stretch zone regions were delimited from elevation maps using a tablet. Each elevation map was divided in three rectangular areas of same size, since the stretch zone was enclosed (Fig. 3). This procedure avoids a large variation on stretch zone width measurements, computed as the mean value for all line segments inside stretch zone. Same rectangular areas were considered for fractal dimension measurements.

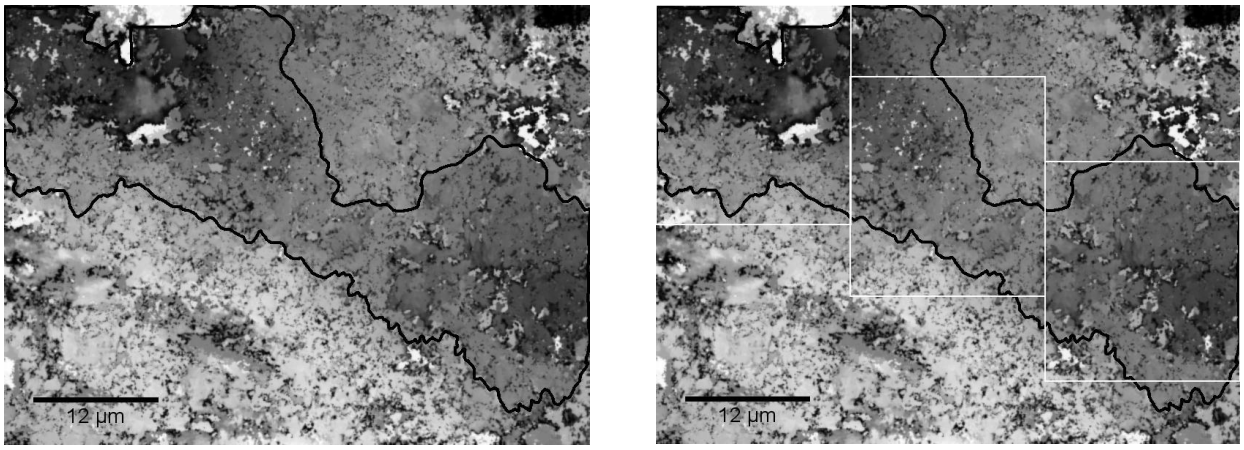

(a) (b)

Figure 3. Stretch zone: a) delimitation of stretch zone; b) sampling procedure for fractal dimension and stretch zone width measurements.

Stretch zone fractal dimension data were computed using another plugin for NIH Image J, the "Map Fractal Count", based on the Minkowski-Bouligand dimension method, also known as box-counting dimension (Chen *et al*, 2003), which systematically lay a series of grids of decreasing box size over the grayscale elevation map and record the number of boxes for each successive grid size, finding the fractal dimension D as the slope of the logarithmic regression line for box numbers and grid sizes.

3. RESULTS AND DISCUSSION

Stretch zone is characterized by a featureless appearance distinguishable from the fatigue surface and the subsequent main fracture by ductile tearing or brittle cleavage (Tarpani *et al.*, 2003). It is sometimes very hard to define its limits, so some criteria must be followed. In general, stretch zone boundaries are characterized by evident relief transitions (Hein *et al.*, 1999), as the first blunting after stable propagation region and the strongly oblique slipping surface, characteristic of stretching mechanism, before dimples formation. These topographic changes can be easily identified from elevation maps, even when are not clearly recognized from reconstructed in-focus images. This affirmative is not correct under severe plane stress state, when extensive plastic strain provokes abrupt and discontinuous changes in local topography, being very imprecise the delimitation of stretch zone regions. In this study, stretch zone measurements from 9.0 mm thick specimens were discarded and only the measurements on central region of 12.7 mm thick specimens were considered, due to the predominance of plane stress state. This procedure provides a reliable delimitation of stretch zone boundaries, being possible to study their heterogeneous geometry. According to Tab. 1, there is a large dispersion on stretch zone width values, especially when the plane strain state is not well established.

Table 1. Stretch zone width dispersion relative to specimen thickness

	Thickness [mm]					
	12.7		15.0		19.0	
	center	edge	center	edge	center	edge
Mean Wsz [µm]	15.99	----	12.92	11.39	13.42	13.39
Standard deviation Wsz [µm]	0.99 (6%)	----	4.01 (31%)	3.11 (27%)	4.15 (31%)	3.96 (30%)
Minimum value Wsz [µm]	14.38	----	7.21	6.67	8.72	5.78
Maximum value Wsz [µm]	17.18	----	17.44	15.34	21.47	17.48

Taking all measured values for stretch zone width and fractal dimension for all analyzed regions in each specimen, it is observed that the correlation coefficients grow with specimen thickness (Fig. 4). The correlation coefficient is larger for 19 mm thick specimens, equals to 0.7983, which is not large enough to provide a reliable correlation between fractal dimension and stretch zone width values. It demonstrates that stretch zone has heterogeneous topographic behavior along thickness, being dependent on local stress fields.

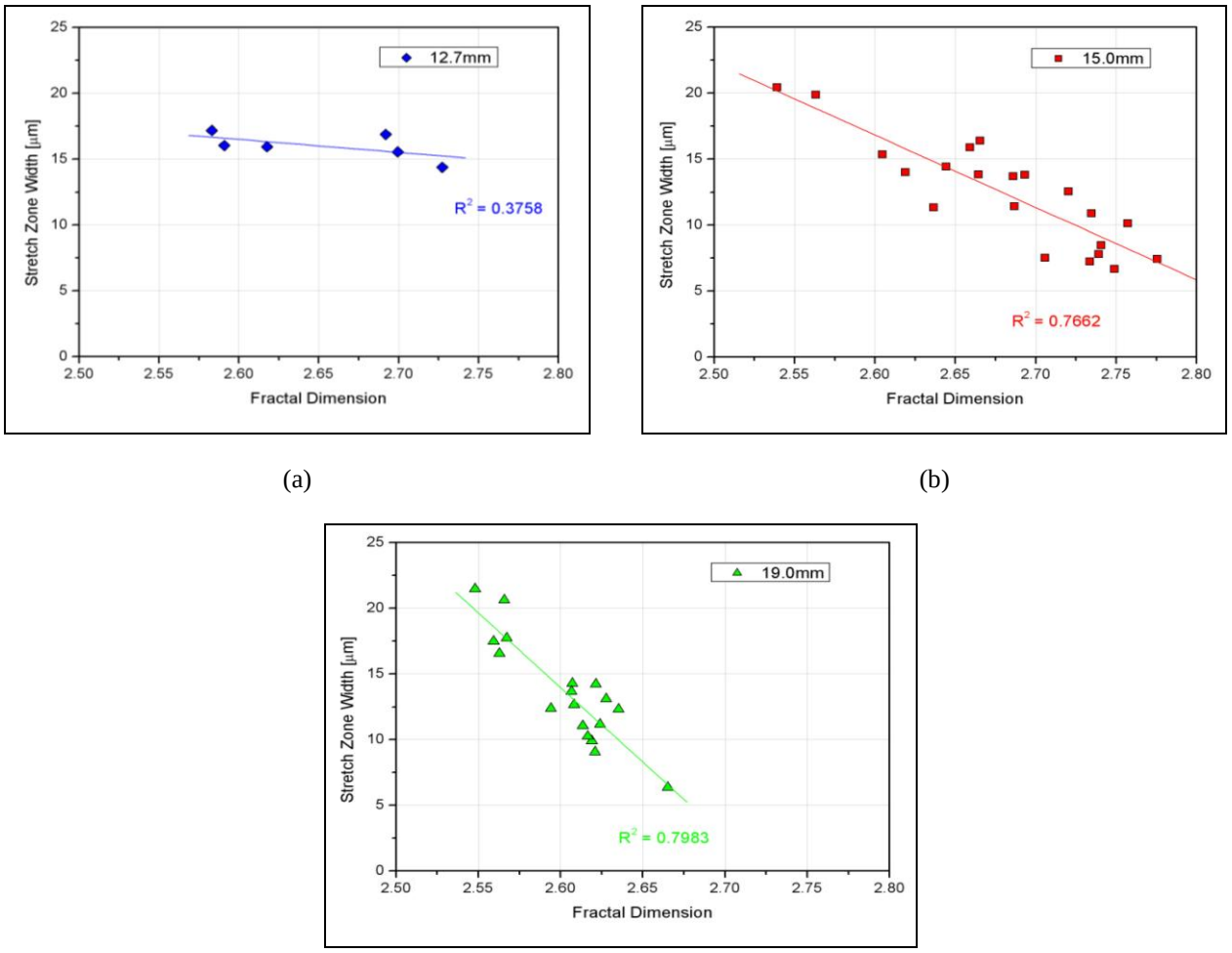

(a) (b)

(c)

Figure 4. Stretch zone width versus fractal dimension graphs for specimens with different thickness. a) 12.7 mm; b) 15.0 mm; c) 19.0 mm

This heterogeneity can be evaluated by separating center (half of plate thickness) and edges (at ¼ and ¾ of plate thickness) information. In Figure 5a, the correlation coefficient for the 12.7 mm thick plate is very low, due to the excessive plastic strain at the center, whereas 15.0 mm and 19.0 mm specimens present progressive and significant correlation between stretch zone width and fractal dimension data. The larger correlation coefficient for 19.0 mm specimen is explained by the better defined plane strain state than in 15.0 mm thick sample. This affirmative is corroborated by Figure 5b, where the correlation coefficients for edges data describe no significant relation between stretch zone and fractal dimension values. At edges, plane strain is not established, and fracture surface is formed by predominant action of tearing and shear stresses, resulting in complex topographies. These data are summarized in Tab. 2.

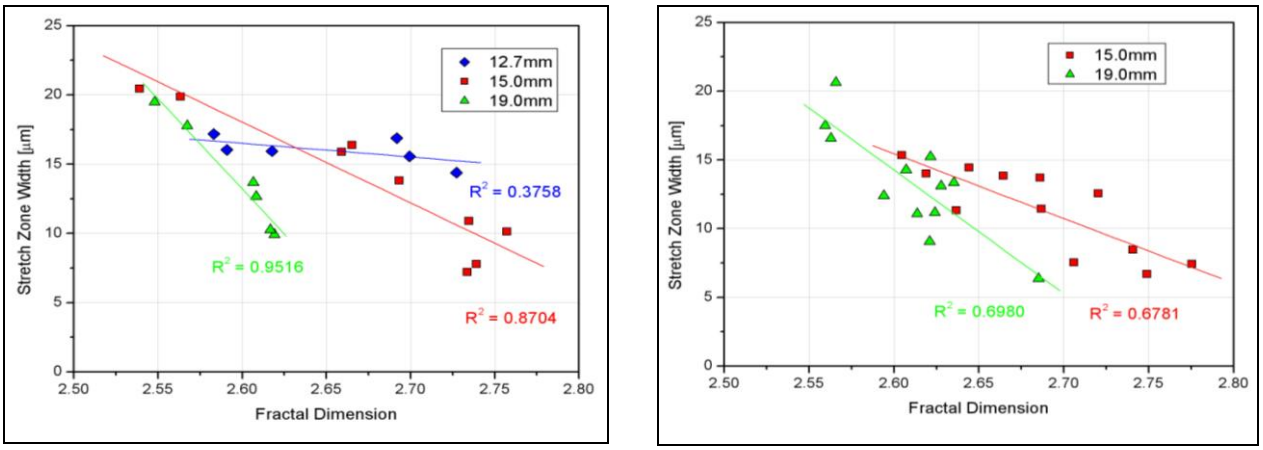

(a) (b)

Figure 5. Stretch zone width versus fractal dimension graphs for all specimens. a) center data; b) near edges values

Table 2. Correlation coefficients and specimen thicknesses

Thickness [mm]	R^2 (center)	R^2 (edge)
12.7	0.3758	----
15.0	0.8704	0.6781
19.0	0.9516	0.698

Linear equations for fractal dimension (D) versus stretch zone width (W_{sz}) were obtained for center data measured for each specimen thickness, as in Figure 5a, and present the general format as in Eq. (1):

$$W_{sz} = aD + b \tag{1}$$

These equations are disposed in Tab. 3. Taking the a and b coefficients in Tab. 3, it was compared their evolution against thickness (t) values, obtaining the graphs in Fig. 6.

Table 3. Linear equations for stretch zone width versus fractal dimension plots

Thickness[mm]	Equation	R^2
12.7	**Wsz** = -9.889***D** + 42.22	0.3758
15.0	**Wsz** = -58.289***D** + 169.59	0.8704
19.0	**Wsz** = -129.950***D** + 351.08	0.9516

As the correlation coefficients for a x t (Eq. 2) and b x t (Eq. 3) were significant (Fig. 6), the Eq. (4) could be obtained by substituting Eq. (2) and (3) in Eq. (1), so:

$$a = -0.0172t + 197.58 \tag{2}$$

$$b = 0.0442t - 489.96 \tag{3}$$

$$W_{sz} = (-0.0172t + 197.58)D + 0.0442t - 489.96 \tag{4}$$

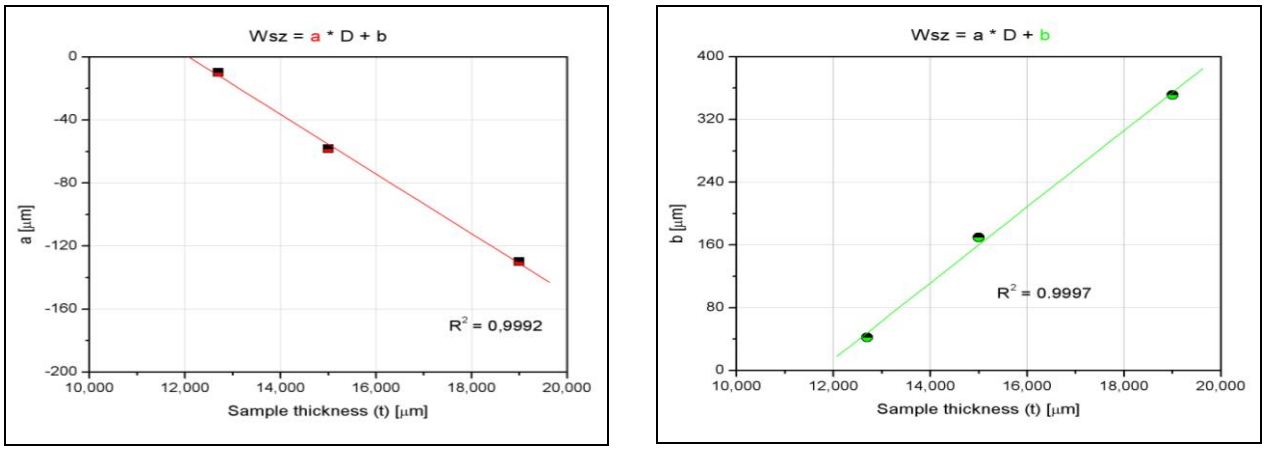

(a) (b)

Figure 6. Linear equations coefficients dependence of specimen thickness. a) a X t; b) b X t

Equation (4) relates the dependence for stretch zone width on both fractal dimension and thickness. It is also noticeable that fractal dimension behavior is also dependent on thickness due to elastic-plastic condition at crack front. Based on these results, it is possible to suggest a general form for the relationship between stretch zone size and fractal dimension under elastic-plastic conditions as:

$$W_{sz} = (c_1 t + c_2)D + c_3 t + c_4 \quad (5)$$

Where c_1 and $c_4 < 0$, and c_2 and $c_3 > 0$. The c_i constants are proposed as material properties, related to microstructure and loading conditions.

4. CONCLUSIONS

The plastic behavior of fracture surfaces is more pronounced near specimen edges due to the existence of plane stress conditions, limiting the significance of their descriptions by fractal dimension values at stretch zone region. The predominance of plane strain states provide better definition of stretch zone formations, reducing the scattering on width measurements and resulting in representative relationships with local fractal dimension, as observed for large thickness specimens. It is suggested a general equation to describe stretch zone width, a local toughness measurement, as a function of fractal dimension and thickness, applied for elastic-plastic states. So, fractal dimension expresses the local toughness behavior and its dependence to the geometry of fractured body under elastic-plastic loading conditions in plane strain region, but it is not a significant descriptor under plane stress state.

5. ACKNOWLEDGEMENTS

This work was supported by FAPESP (Fundação de Amparo à Pesquisa do Estado de São Paulo), under grant numbers 2008/01788-2 and 2001/ 09664-1 and CNPq (Conselho Nacional de Desenvolvimento Científico e Tecnológico), under processes 307271/2007-2 and 471749/2008-7.

6. REFERENCES

ASTM, 2008, "E1290-08: Standard Test Method for Crack-Tip Opening Displacement (CTOD) Fracture Toughness Measurement", Annual Book of ASTM Standard, Vol.3.01.

Balakin, A.S., 1997, "Physics of fracture and mechanics of self-affine cracks", Eng. Fract. Mech., Vol.57, pp. 135-203.

Charkaluk, E., Bigerelle, M., Iost, A., 1998, "Fractals and fracture", Eng. Fract. Mech., Vol.61, pp. 119-139.

Chen, W., et. al., 2003, "Two algorithms to estimate fractal dimension of gray level images", Optical Eng., Vol.42, pp. 2452-2464.

Das, S.K., Sivaprasad, S., Das, S., Chatterjee, S., Tarafder, S., 2006, "The effect of variation of microstructure on fracture mechanics parameters of HSLA-100 steel", Mat. Sci. Eng. A, Vol.431, pp. 68–79.

Forster, B., et. al., 2004, "Complex Wavelets for Extended Depth-of-field: A new method for the fusion of multichannel microscopy images", Microsc. Res. Tech., Vol.65, pp. 33-42.

Goldsmith, N.T., 2000, "Deep focus: a digital image processing technique to procedure improved focal depth in light microscopy", Image Anal. Stereol., Vol.19, pp. 163-167.
Hein, L.R.O., Ammann, J.J., Nazar, A.M.M., 1999, "Boundary identification criteria and geometry analysis of Al 7050 stretch zone from elevation profiles", Mater. Charact., Vol.43, pp. 21-26.
Horovistiz, A.L., et. al., 2003, "Quantitative fractography under light microscopy: a digital image processing approach", Prakt. Metallogr., Vol.40, pp. 57-68.
Horovistiz, A.L., Hein, L.R.O., 2005, "Fractal analysis along stretch zone for an aluminum alloy", Mater. Lett., Vol.59, pp. 790-794.
Landes, J.D., 1995, "Blunting line in elastic-plastic fracture", Fat. Fract. Eng. Mater. Struct., Vol.18, pp. 1289-1297.
Pandey, R.K., Sundaram, P., Kumar, A.N., 1991, "A stretch zone method for ctod evaluation", Int. Journal Fract., Vol.47, pp. R29-R32.
Prudencio, A., et.al., 2009, < http://bigwww.epfl.ch/demo/edf/index.html>, Ecole Polytechnique Fédérale de Lausanne.
Ranganath, V.R., Pandey, R.K., Kumar, A.N., 1990, "A comparative study of various approaches for ctod toughness evaluation", Eng. Fract. Mech., Vol.37, pp.1059-1069.
Rasband, W.S., 2008, "ImageJ", U. S. National Institutes of Health, Bethesda, Maryland, USA, <http://rsb.info.nih.gov/ij/>.
Stach, S., Cybo, J.J., Chmiela, J., 2001, "Fracture surface – fractal or multifractal?", Mater. Charact., Vol.46, pp. 163-167.
Tarpani, J.R., Bose, W.W., Spinelli, D., 2003, "Backscattered electron microscopy technique enhancing stretch zone width imaging for initiation fracture toughness measurements", Mater. Charact., Vol.51, pp. 159-170.

7. RESPONSIBILITY NOTICE

The authors are the only responsible for the printed material included in this paper.